

## Rigidity Loss in Disordered Systems: Three Scenarios

Wouter G. Ellenbroek,<sup>1</sup> Varda F. Hagh,<sup>2</sup> Avishek Kumar,<sup>2</sup> M. F. Thorpe,<sup>2,3</sup> and Martin van Hecke<sup>4,5</sup>

<sup>1</sup>*Department of Applied Physics and Institute for Complex Molecular Systems, Eindhoven University of Technology, Postbus 513, NL-5600 MB Eindhoven, The Netherlands*

<sup>2</sup>*Department of Physics, Arizona State University, Tempe, Arizona 85287-1504, USA*

<sup>3</sup>*Rudolf Peierls Centre for Theoretical Physics, University of Oxford, 1 Keble Road, Oxford OX1 3NP, England*

<sup>4</sup>*Huygens-Kamerlingh Onnes Lab, Universiteit Leiden, P.O. Box 9504, NL-2300 RA Leiden, The Netherlands*

<sup>5</sup>*FOM Institute AMOLF, Science Park 104, 1098 XG Amsterdam, The Netherlands*

(Received 28 November 2014; revised manuscript received 2 March 2015; published 1 April 2015)

We reveal significant qualitative differences in the rigidity transition of three types of disordered network materials: randomly diluted spring networks, jammed sphere packings, and *stress-relieved* networks that are diluted using a protocol that avoids the appearance of floppy regions. The marginal state of jammed and stress-relieved networks are globally isostatic, while marginal randomly diluted networks show both overconstrained and underconstrained regions. When a single bond is added to or removed from these isostatic systems, jammed networks become globally overconstrained or floppy, whereas the effect on stress-relieved networks is more local and limited. These differences are also reflected in the linear elastic properties and point to the highly effective and unusual role of global self-organization in jammed sphere packings.

DOI: 10.1103/PhysRevLett.114.135501

PACS numbers: 62.20.D-, 63.50.Lm, 64.60.ah

Disordered elastic networks and sphere packings represent a large class of amorphous athermal materials, ranging from (bio)polymer networks to granular media and foams [1–3]. Random networks of springs lose their rigidity when enough springs are cut; this random bond dilution process is known as rigidity percolation (RP) [4–8]. Packings of soft spheres do the same when their confining pressure is lowered towards zero: This is called (un)jamming [9–13]. These rigidity loss scenarios have been studied extensively, in particular, for the simplest cases of networks of harmonic springs [7,8] or soft frictionless harmonic spheres [10–13]. In that case, the linear elastic properties of packings can be mapped to those of a spring network, where each contact is replaced by the appropriate spring [14–16]. Lowering the pressure, the number of bonds in the equivalent network decreases.

Given this close correspondence, it is surprising that the nature of the RP and unjamming transitions, and of their respective marginally rigid states, are significantly different. For packings of a large number ( $N$ ) of soft spheres, extensive studies have shown that (i) the connectivity, i.e., the average number of contacts  $z$  per particle, goes to  $z_c = 2D + \mathcal{O}(1/N)$  at the marginal point, where  $D$  is the space dimension [3,9–13,17–20], (ii) the system remains homogeneously jammed up to the point of unjamming (with the exception of individual loose particles called rattlers or very rare small particle clusters) [10], and (iii) the shear modulus  $G$  vanishes as  $\Delta z := z - z_c$  whereas the bulk modulus  $K$  remains finite when  $\Delta z \rightarrow 0$  [9–14]. In contrast, in the rigidity percolation of generic networks, extensive studies have revealed that for large systems (i) the connectivity  $z$ , which gives the average number of springs per

node, approaches  $z_c = 3.9612\dots < 2D$  for the bond diluted triangular network [7,8], (ii) the largest rigid cluster takes on a heterogeneous, fractal shape, and (iii) both the shear modulus  $G$  and bulk modulus  $K$  smoothly vanish at the critical point in a way typical for a second order phase transition [7,8].

To understand these differences, we note that the small difference in  $z_c$  points to a huge, qualitative difference between jammed and random networks. Based on extensions of the ideas of Maxwell [21], a simple mean field argument locates the marginal point where the number of degrees of freedom ( $DN$  coordinates) is balanced by the number of constraints ( $zN/2$  bonds) at  $z = 2D$ . This argument is exact if all the constraints are independent and there is a single rigid cluster. If there are redundant bonds,  $z_c$  can deviate from  $2D$ , although proper counting of *actual* degrees of freedom and *independent* constraints would remove this apparent violation of Maxwell's criterion [22]. Indeed, the rigid network in RP contains both redundant constraints (bonds) and flexible hinges (sites) at the marginal point so that  $z_c \neq 2D$ . In contrast, we will show that sphere packings at the jamming transition are isostatic everywhere: Nothing can move (except a few rattlers) and *every bond is essential* for the rigidity of the network. Jammed systems show a high degree of organization, leading to highly nongeneric networks [16].

Several open questions thus arise: What is different in the topology and geometry of the underlying networks of random springs and jammed packings? Can we conceive other families of networks with different rigidity loss transitions? Here we address these questions by determining the overconstrained and underconstrained regions using

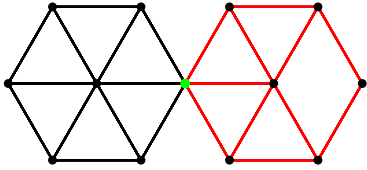


FIG. 1 (color online). Rigid region decomposition, where there are two rigid regions, one (black bonds) overconstrained and the other isostatic (red bonds), separated by a hinge (light green site). The sites which are not hinges are colored black.

the pebble game [7,8]. This is an integer algorithm that analyzes the topology of generic spring networks, by a very effective decomposition of such networks into rigid regions, with both unstressed (isostatic) and stressed (overconstrained or superfluous [23]) rigid regions, and the hinges that separate rigid regions.

Figure 1 illustrates such an analysis for a small network. The 12 black bonds (Fig. 1, left) might carry finite forces while maintaining force balance: Such bonds are redundant, as any one of these bonds could be removed and the remainder would still be rigid, and are called *stressed*. We emphasize that a stressed bond typically, but not necessarily, carries a finite force: The concept of stressed or redundant bonds should not be confused with, e.g., the prestress [16,24]. The 11 red bonds (Fig. 1, right) show a rigid cluster that is exactly isostatic, and removal of any of these bonds would break the cluster. Such bonds are called unstressed, and necessarily carry zero force. Finally, the green node in the center of this network is a hinge (defined as a site that belongs to at least two rigid clusters). For more complex networks, the pebble game is an effective algorithm to unambiguously determine the rigid clusters [7,8].

*Pebble game analysis.*—We will now characterize three families of network topologies by the pebble game. Unless otherwise stated RP will refer to the *bond diluted triangular network* in this Letter, which is the best studied system. For all networks, we use periodic (wrap-around) boundary conditions.

Figure 2 shows dramatic differences in the nature of the marginal states depending on the physical process that generates these networks. The top row shows a jammed-packing-derived network at the marginal state (center), one contact above it (right) and one contact below (left), obtained by randomly removing bonds from a very weakly jammed packing ( $z < 4.01$ ). Strikingly, in the marginal state of the jammed network, all bonds are isostatic (red), just above it, the whole system is overconstrained (black), and when a single bond is removed, almost every site becomes a hinge (green). In terms of the network topology, this is a massively first order transition. In the bottom row of Fig. 2, the gentle evolution through the marginal state in RP is shown. The marginal state contains both isostatic and redundant pieces in the percolating rigid backbone, as well as significant numbers of green hinges—adding or

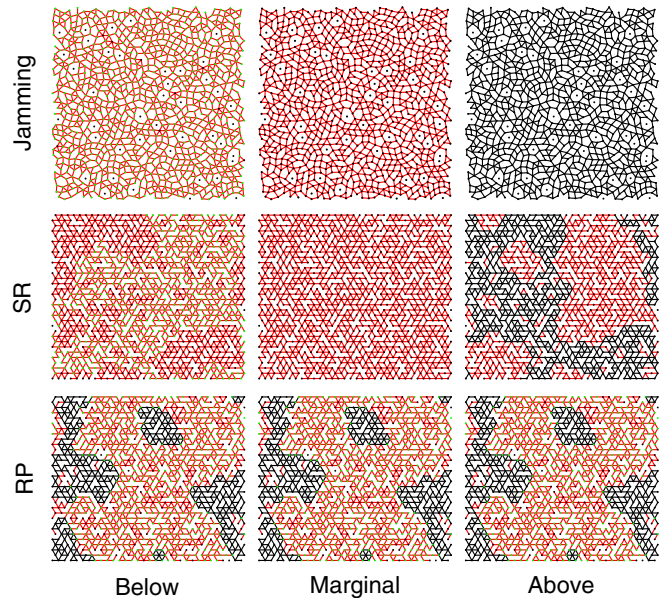


FIG. 2 (color online). Pebble game results for a jammed packing (top row), a stress-relieved triangular network (middle row), and rigidity percolation (bottom row). The center panel is the marginal case in all three panels, with the left panel having a single bond removed and the right panel a single bond restored. The marginal states of both jammed systems as well as the SR network is fully isostatic (red), whereas the marginal state for RP features floppy modes (involving the light green hinge sites) and has 34% of all bonds stressed (black).

removing a single bond hardly changes the configuration, typical of a second order transition.

We now introduce a third family of networks that becomes isostatic everywhere at their marginal point—as in jamming—by cutting bonds randomly, but only if they are stressed. This stress-relieving (SR) cutting algorithm leads, by construction, to the percolating marginally rigid cluster being *precisely and exactly isostatic* everywhere, without any overconstrained or underconstrained regions. This also means that in both jamming and SR (but not RP) the transition happens at the mean field Maxwell point, so that the mean coordination is  $2D$  with zero redundant constraints anywhere.

In the middle row of Fig. 2 we show the pebble game analysis for SR cutting, starting from a triangular network. An isostatic state with a single cluster is produced at the marginal point, reminiscent of the jammed state. However, this marginal state is very different in character: Both adding or removing a bond has a less dramatic effect than in jamming. Hence, isostaticity everywhere is not the only nontrivial feature of the jammed state: Its organization is such that its globally isostatic state is changed *everywhere* by the addition or subtraction of a *single constraint*, in stark contrast to SR networks.

Both stressed and random bond removal can be performed on any initial configuration, including jamming-derived networks at given connectivity  $z_j$ . Doing so yields

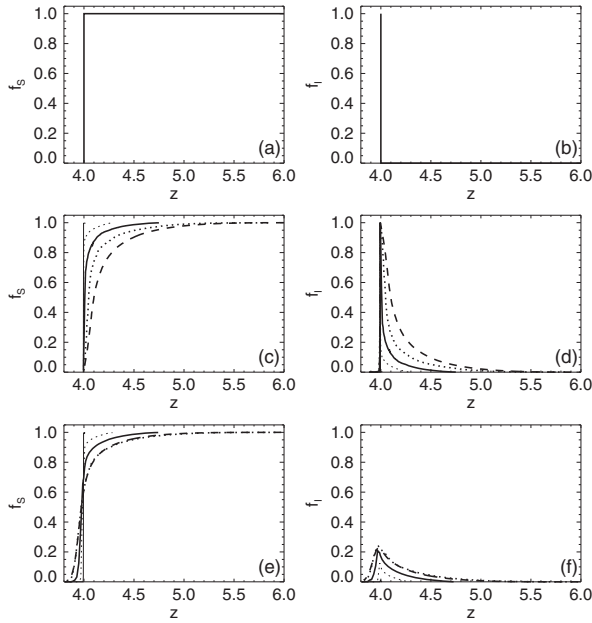


FIG. 3. Fraction of stressed (left) and isostatic (right) bonds in the rigid backbone for jamming (top), stressed bond dilution (middle), and random bond dilution (bottom). In (c)–(f), line styles indicate the starting point for bond removal: jammed networks at  $z_j = 4.01$  (solid, thin),  $z_j = 4.3$  (dotted, thin),  $z_j = 4.7$  (solid, thick),  $z_j = 5.98$  (dotted, thick), and triangular (dashed, thick). Data are averaged over 300 triangular nets or 25–50 jamming-derived networks.

two two-parameter families of networks, each characterized by  $z$  and  $z_j$ . Starting with  $z_j$  close to  $2D$ , we can, for example, probe how, and how quickly, the network topology crosses over from jammed to generic or SR-like.

In Fig. 3 we compare the fractions of stressed and isostatic bonds for jamming (top row), SR (middle row), and RP (bottom row), where the latter two have initial configurations corresponding to jammed networks at four different values of  $z$  or a triangular net. For jamming, the fraction of stressed bonds  $f_s$  discontinuously jumps from one to zero, and the fraction of isostatic bonds  $f_i$  jumps from zero to one when  $z$  is lowered, consistent with the picture shown in Fig. 2. This happens because in jammed sphere packings only contacts that carry a positive force can be detected and therefore all bonds in the network must be stressed. For *random* bond dilution,  $f_s(z)$  and  $f_i(z)$  remain continuous irrespective of  $z_j$ , and for large  $z_j$ , these functions smoothly approach those of the triangular net.

In the middle row of Fig. 3 we show  $f_s(z)$  and  $f_i(z)$  for the same five families of networks for *stressed* bond dilution. The data shown here appear to have a discontinuity around  $z = 4$ ; it is an open question whether this discontinuity persists in the thermodynamic limit. For  $z_j = 5.98$ , the apparent jump is small, and the curves are closer to those of the triangular net. However, we still see deviations from the triangular case, which is surprising

given that here we have to cut almost 1/3 of the bonds to reach the critical point. For smaller  $z_j$ , the apparent jumps in  $f_s$  and  $f_i$  grow, approaching the step functions of jamming—this is easy to understand, as for  $z_j \rightarrow 4$  an increasingly small fraction of bonds gets removed before reaching  $z = 4$ .

*Discontinuous response to bond addition and removal.*—The response to the addition or removal of bonds is a measure for the degree of organization in the network, and to quantify the discontinuous response at the marginal point more precisely, we introduce two new indices. The first is  $h$ , the ease-of-breakup index which is defined by removing one bond randomly from the marginal state, counting the number of new green hinges, averaging over every bond in the network, and dividing by the number of sites so that  $0 < h < 1$ . The second is  $s$ , the ease-of-stressing index, defined by adding one bond randomly, counting the number of new stressed bonds, averaging over all bonds and dividing by the number of bonds so that  $0 < s < 1$ . High values of  $h$  and  $s$  imply strong self-organization of the network.

We find that in networks representing packings near unjamming the index  $h \approx 0.97$  and  $s \approx 0.98$  (cf. top row of Fig. 2), while for RP networks, both indices are very small ( $h \approx 0.0003$  and  $s \approx 0.001$ ) as expected for a second order transition (see Fig. 2). Intermediate values of  $h$  and  $s$  are found for SR ( $h \approx 0.28 \pm 0.04$  and  $s \approx 0.47 \pm 0.05$ ), where the spread is specific to our system sizes and is expected to go down for larger systems. We have made an additional isostatic marginal state by adding bonds to an empty triangular net, avoiding adding stressed bonds, which also produces a marginal isostatic state, but with even lower index values:  $h \approx 0.21$  and  $s \approx 0.40$ . The large values of both  $h$  and  $s$  for the jammed state show how remarkably self-organized it is.

To understand the large  $h$  index for jamming, we start from the globally isostatic jammed network at the critical point: According to Laman’s theorem [25], the number of bonds equals  $2N - 3$  and the number of bonds  $b$  in subgraphs of  $n$  nodes satisfies  $b \leq 2n - 3$ . After we remove a bond, only subgraphs that have precisely  $2n - 3$  bonds are isostatic. Examples of these are  $n = 3$  triangles or  $n = 4$  double triangles (Fig. 2). Here all nodes are at the cluster’s edge and are hinges; “black dots” can only arise in the interior of isostatic clusters. The large value of  $h$  thus implies that  $n > 4$  isostatic clusters are rare in jamming, compared to SR and RP.

We now suggest that large  $n$  isostatic clusters are suppressed due to the homogeneity of jammed systems, using a variation on a well-known bond cutting argument [11,12,26,27]. Consider a large (hypothetical) isostatic cluster  $C$  with  $n$  nodes and  $2n - 3$  internal connections, and  $n_e$  nodes at the edge of  $C$ . All  $\mathcal{O}(n_e)$  connections that cross the boundary of  $C$  (for SR and RP there may be fewer) do not contribute to internal connections, so that the

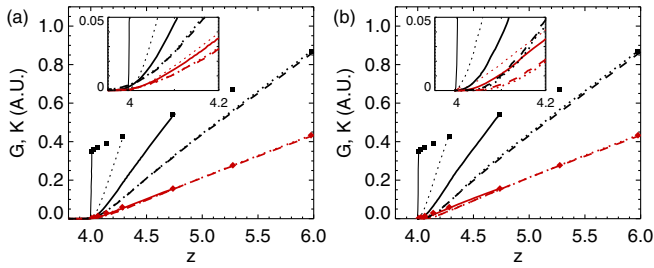


FIG. 4 (color online). Shear modulus  $G$  (red) and bulk modulus  $K$  (black) for (a) random bond dilution and (b) stressed bond dilution. As in Fig. 3, the initial condition is the network of a jammed packing at  $z_j = 4.01$  (solid, thin),  $z_j = 4.3$  (dotted, thin),  $z_j = 4.7$  (solid, thick),  $z_j = 5.98$  (dotted, thick), and triangular networks (dashed, thick) as the initial condition. Insets show zoom ins around the transition. Solid squares and diamonds denote the moduli of the jammed packings as published earlier in Ref. [16].

mean contact number of  $C$  is  $4 + \mathcal{O}(n_e/n)$ —as  $n_e \sim \sqrt{n}$ , this is significantly above the global mean contact number 4, even for relatively large clusters (for a  $n = 100$  circular cluster we estimate  $z \approx 4.3$ ). Whereas RP and SR systems below the marginal point clearly have such subgraphs, these become extremely unlikely for jammed systems. Thus, the  $h$  index in jamming is much larger than in SR or RP because spatial fluctuations in local contact numbers are smaller [28]. How precisely this homogeneity arises remains an open problem.

To understand the large  $s$  index for jamming, we note that for jammed networks, all bonds carry a positive force and are stressed, as jammed systems are at finite pressure. For SR and RP networks there is no positivity condition on the contact forces, and both isostatic zero force regions and stressed regions where positive and negative forces precisely balance can occur. This difference is clearly illustrated in SR and RP networks above the marginal point, where stressed regions can have convex edges where forces of opposite sign balance—this is ruled out in jamming. We believe that such differences also underlie the inequality of the  $s$  index for jamming and SR.

*Elastic moduli.*—We calculate the elastic moduli of the networks in linear response from the dynamical matrix [29–31]. In Fig. 4 we show shear ( $G$ ) and bulk ( $K$ ) moduli as a function of  $z$  for the same four values of  $z_j$  as in Fig. 3 and for the generic triangular net, both for random bond dilution and for stressed-bond-only dilution. Clearly, a very simple scenario unfolds: (1) For  $z_j \approx 6$ , the functions  $G(z)$  and  $K(z)$  are virtually identical to those for the bond dilution of triangular nets. (2)  $G(z)$  is essentially independent of  $z_j$ , consistent with our earlier observations [16]. (3) The behavior of  $K$  is richer. For jammed networks with  $z = z_j$ ,  $K$  weakly depends on  $z$  but remains finite [ $K_j(z = 4) > 0$ ]. However, for all  $z_j$  that we have investigated, we find that upon bond dilution  $K$  vanishes as

$$K(z, z_j) = K_j(z_j)[(z_j - z)/(z_j - z_c)]^\alpha, \quad (1)$$

where  $\alpha$  is close to unity. Our systems are too small to precisely determine  $\alpha$ , although the smoothing near  $z = 4$  is consistent with  $\alpha \approx 1.4$  as found for 2D triangular nets.

Is this difference in moduli related to  $h$  and  $s$ ? Strictly speaking, no: It is the network’s geometry, not topology, which determines the elastic response (even small geometric perturbations of networks, be they quasicrystals [32] or jammed [33], can strongly perturb  $K$ ). However, both the large value of  $s$  and the finite value of  $K$  are intimately connected to the repulsive nature of contacts in jamming [14,16,32]. Clearly the network reorganizations of jammed systems when they are decompressed (such geometric reorganizations are absent in SR and RP) leads to networks where finite positive contact forces can balance, and  $h$  and  $s$  tend to one.

*Discussion.*—It was known that jammed networks had to satisfy the Maxwell condition globally and had to satisfy the Hilbert criterion locally [2], but neither of those imply the self-organization in terms of rigid cluster analysis that we uncover. From a design perspective, our two-parameter families of networks are attractive because they allow us to independently set the ratio  $G/K$  of elastic moduli and the connectivity  $z$  (Fig. 4). Fully random networks are non-optimal in propagating rigidity, as unhelpful stressed regions remain in the backbone. SR networks are better, but still become soft against compression at their marginal point. Jamming can be seen as a strategy to find special, perhaps optimal geometries of spring networks in terms of propagating rigidity and resistance to compression, although jammed networks are not the only ones that have finite  $K$  at the marginal point [32]. We have not been able to come up with algorithms that generate networks with the same intricate network topologies as jamming, and suggest that whether this is possible remains an important open problem [34,35].

Finally, many other marginal networks have been studied recently [36–38]. Square and kagome lattices with randomly added braces, which are even more homogeneous than jammed networks, were shown to also have a very sharp rigidity transition [39] with (in our terminology)  $h$  and  $s$  close to 1, consistent with our findings. One alternative protocol to create networks that are isostatic everywhere was introduced by Lopez *et al.* [35]. For small  $N$ , these networks become macroscopically floppy upon the removal of a single bond, but this effect disappears as  $N$  increases, and we expect that their networks are similar to our SR networks, with  $K \rightarrow 0$ . Another recent conditional cutting protocol allows for the independent tuning of the ratio of bulk and shear moduli [40]. We hope that our work will inspire work to analyze such network topologies, leading to better understanding which other families of networks can be constructed, with distinct properties of the

stressed and isostatic bonds, hinges,  $h$  and  $s$  indices, and elastic moduli.

We acknowledge discussions with N. Upadhyaya and V. Vitelli, who did early calculations on the bulk modulus in a two-parameter family of networks. W. G. E. acknowledges support from NWO/VENI. M. v. H. acknowledges support from NWO/VICI. The work at Arizona State University was supported by the National Science Foundation under Grant No. DMR 0703973NSF. A. K. would like to acknowledge funding from GAANN P200A090123 and the ARCS Foundation.

- 
- [1] C. P. Broedersz and F. C. MacKintosh, *Rev. Mod. Phys.* **86**, 995 (2014).
- [2] S. Alexander, *Phys. Rep.* **296**, 65 (1998).
- [3] D. J. Durian, *Phys. Rev. E* **55**, 1739 (1997).
- [4] S. Feng and P. N. Sen, *Phys. Rev. Lett.* **52**, 216 (1984).
- [5] S. Feng, M. F. Thorpe, and E. Garboczi, *Phys. Rev. B* **31**, 276 (1985).
- [6] M. Sahimi, *Phys. Rep.* **306**, 213 (1998).
- [7] D. J. Jacobs and M. F. Thorpe, *Phys. Rev. Lett.* **75**, 4051 (1995).
- [8] D. J. Jacobs and M. F. Thorpe, *Phys. Rev. E* **53**, 3682 (1996).
- [9] A. J. Liu and S. R. Nagel, *Nature (London)* **396**, 21 (1998).
- [10] C. S. O'Hern, L. E. Silbert, A. J. Liu, and S. R. Nagel, *Phys. Rev. E* **68**, 011306 (2003).
- [11] M. van Hecke, *J. Phys. Condens. Matter* **22**, 033101 (2010).
- [12] A. J. Liu and S. R. Nagel, *Annu. Rev. Condens. Matter Phys.* **1**, 347 (2010).
- [13] C. P. Goodrich, S. Dagois-Bohy, B. P. Tighe, M. van Hecke, A. J. Liu, and S. R. Nagel, *Phys. Rev. E* **90**, 022138 (2014).
- [14] M. Wyart, *Ann. Phys. (Paris)* **30**, 1 (2005).
- [15] M. Wyart, H. Liang, A. Kabla, and L. Mahadevan, *Phys. Rev. Lett.* **101**, 215501 (2008).
- [16] W. G. Ellenbroek, Z. Zeravcic, W. van Saarloos, and M. van Hecke, *Europhys. Lett.* **87**, 34004 (2009).
- [17] C. F. Moukarzel, *Phys. Rev. Lett.* **81**, 1634 (1998).
- [18] A. V. Tkachenko and T. A. Witten, *Phys. Rev. E* **60**, 687 (1999).
- [19] S. Dagois-Bohy, B. P. Tighe, J. Simon, S. Henkes, and M. van Hecke, *Phys. Rev. Lett.* **109**, 095703 (2012).
- [20] C. P. Goodrich, A. J. Liu, and S. R. Nagel, *Phys. Rev. Lett.* **109**, 095704 (2012).
- [21] J. C. Maxwell, *Philos. Mag.* **27**, 294 (1864).
- [22] C. Calladine, *Int. J. Solids Struct.* **14**, 161 (1978).
- [23] M. Thorpe, D. Jacobs, M. Chubynsky, and J. Phillips, *J. Non-Cryst. Solids* **266–269**, 859 (2000).
- [24] M. Wyart, L. E. Silbert, S. R. Nagel, and T. A. Witten, *Phys. Rev. E* **72**, 051306 (2005).
- [25] G. Laman, *J. Eng. Math.* **4**, 331 (1970).
- [26] M. Wyart, S. R. Nagel, and T. A. Witten, *Europhys. Lett.* **72**, 486 (2005).
- [27] C. P. Goodrich, W. G. Ellenbroek, and A. J. Liu, *Soft Matter* **9**, 10993 (2013).
- [28] S. Henkes, K. Shundyak, W. van Saarloos, and M. van Hecke, *Soft Matter* **6**, 2935 (2010).
- [29] F. Leonforte, A. Tanguy, J. P. Wittmer, and J.-L. Barrat, *Phys. Rev. B* **70**, 014203 (2004).
- [30] W. G. Ellenbroek, E. Somfai, M. van Hecke, and W. van Saarloos, *Phys. Rev. Lett.* **97**, 258001 (2006).
- [31] W. G. Ellenbroek, M. van Hecke, and W. van Saarloos, *Phys. Rev. E* **80**, 061307 (2009).
- [32] O. Stenull and T. C. Lubensky, *Phys. Rev. Lett.* **113**, 158301 (2014).
- [33] B. Florijn and M. van Hecke (unpublished).
- [34] L. Yan and M. Wyart, *Phys. Rev. Lett.* **113**, 215504 (2014).
- [35] J. H. Lopez, L. Cao, and J. M. Schwarz, *Phys. Rev. E* **88**, 062130 (2013).
- [36] C. P. Broedersz, X. Mao, T. C. Lubensky, and F. C. MacKintosh, *Nat. Phys.* **7**, 983 (2011).
- [37] K. Sun, A. Souslov, X. Mao, and T. C. Lubensky, *Proc. Natl. Acad. Sci. U.S.A.* **109**, 12369 (2012).
- [38] X. Mao, O. Stenull, and T. C. Lubensky, *Phys. Rev. E* **87**, 042602 (2013).
- [39] L. Zhang, D. Z. Rocklin, B. G. Chen, and X. Mao, *Phys. Rev. E* **91**, 032124 (2015).
- [40] C. P. Goodrich, A. J. Liu, and S. R. Nagel, *arXiv*: 1502.02953.